SECOND EUROPEAN CONFERENCE ON EARTHQUAKE ENGINEERING
AND SEISMOLOGY, ISTANBUL AUG. 25-29, 2014

ON THE RELATION BETWEEN THE NEAR COLLAPSE LIMIT STATES AT THE ELEMENT AND STRUCTURE LEVEL

Klemen REJEC[1] and Peter FAJFAR[2]

ABSTRACT

A generally accepted definition of the near collapse (NC) limit state at the structure level is missing. Two possible candidates are: (1) a 20% drop of the lateral resistance of the structure; (2) the NC limit state of the most exposed important vertical element. The first definition, which seems to be the most appropriate, cannot be applied in non-linear dynamic analysis and also not in pushover analyses with simplified models. The aim of the study presented in this paper is to investigate the relation between the NC limit states defined by the two definitions. Pushover analyses of a significant number of RC structures were performed up to their NC limit state, defined with 20% drop of the strength of the structure. The set of analysed structures included frames, wall systems and a dual system designed according to Eurocode 8, as well as frames designed according to old codes. The results indicate that, in general, the first definition of the NC limit state yields more conservative results than the second definition. 20% drop of lateral resistance of the structure generally occurs at smaller deformation than the 20% drop of the lateral resistance of the most exposed vertical structural element. The difference increases with the height of the structure due to the influence of the second order theory (P-Δ effect).

INTRODUCTION

Collapse prevention is the main objective of any design. Adequate safety margin against collapse under the expected maximum seismic load should be assured. However, it is extremely difficult to predict the physical collapse which involves large deformations, significant second-order effects, and a complex material degradation due to localized phenomena. A number of analytical and experimental studies have been done on this problem. A state of the art on methods to assess the seismic collapse capacity of building structures was prepared by Villaverde (2007). An example of an experimental study was presented by Lignos et al. (2011). In spite of considerable research efforts methods for a reliable assessment of the collapse are not yet available. In practice, often the near collapse (NC) limit state is used as a conservative approximation of the structural collapse. The NC limit state of an individual structural element is usually defined as the point on its pushover curve, at which the horizontal resistance drops for 20% (Figure 1-a). At the level of the structure, a commonly accepted definition of the NC limit state does not exist. An option is a similar definition as in the case of individual elements, i.e. at a 20% drop of the lateral resistance of the structure (Figure 1-b). However, this definition, which seems to be the most appropriate, cannot be applied in non-linear dynamic analysis and also not in pushover analyses with simplified models, e.g. in the case of models without strength-degradation. A more practical definition is based on the assumption that the NC limit state of the structure is reached when the first important vertical element reaches the NC limit state. The aim of the study presented in this paper is to investigate the relation between the NC limit state at the level

[1] PhD, Faculty of Civil and Geodetic Engineering, University of Ljubljana, klemen.rejec@fgg.uni-lj.si
[2] Professor, Faculty of Civil and Geodetic Engineering, University of Ljubljana, peter.fajfar@fgg.uni-lj.si

of the most critical element, which determines the latter definition of the NC limit state at the level of the structure, and the NC limit state of the whole structure according to the first definition.

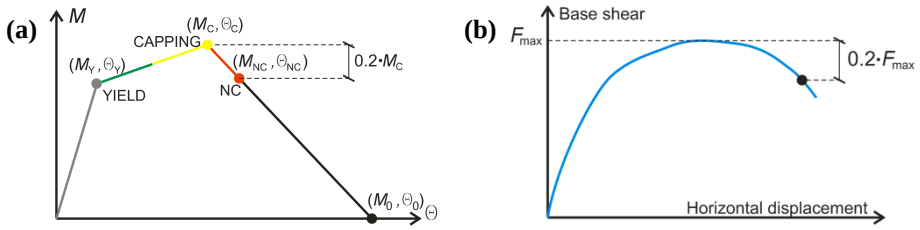

Figure 1. Definition of near collapse (NC) limit state at (a) element and (b) structure level

The damage state of a large number of reinforced concrete (RC) structures, loaded up to the NC limit state, was investigated in a study, recently done at the University of Ljubljana. The set of analysed structures included frames, wall systems and a dual system designed according to Eurocode 8 (CEN, 2005a), as well as frames designed according to old, obsolete codes. The present paper describes the notion, the implementation and the results of the study. First, the characteristics of the analysed structures are described. Then, their computational models, definition of limit states and methods of analyses are presented. Further, a detailed description of damages at NC is given for some representative structures. The most important common characteristics of damage patterns for each individual type of structure are listed. Lastly, the influence of second order effect (P-Δ effect) on the relation between the element and structure NC is explained.

Some assumptions and simplifications were made in the study, which restrain the area of the validity of the results: (i) The analysed structures are idealised representations of real buildings; (ii) Inelastic shear behaviour of elements (which may be important for old structures) is not covered in the computational models; (iii) Moment-rotation characteristics of plastic hinges in the models are represented the by tri-linear backbones with softening (figure 1-b). Due to the lack of empirical data, the slope of the degrading part (softening) could not be defined with confidence; (iv) The method of analysis (basic pushover analyses) does not consider the influence of higher modes.

OVERVIEW OF THE ANALYSED STRUCTURES

The set of analysed structures included frames, wall systems and dual systems designed according to modern codes, as well as frames designed according to old, obsolete codes. Only reinforced concrete structures were investigated. Nevertheless, the findings of the study can be applied for modern steel frames too, since the requirements for local and global ductility are similar. The details of the addressed structures, including some figures, are presented in the next paragraphs.

Frames designed according to modern codes

Six frames designed according to Eurocode 8 were addressed in the study. The frames were designed by Kosič et al. (2014). The set includes specimens having 2 to 8 storeys. Four of them are planar and two spatial. Their notation, details about geometry and notation of analyses are shown in Table 1. The spatial frames were analysed in both orthogonal planes, therefore a total of 8 analyses were performed (noted with consecutive numbers from 1 to 8 in Table 1).

Table 1. Characteristics of frames designed according to modern codes

Specimen notation	*Numb. of storeys*	*Storey height [m]*	*Planar / spatial*	*Direction*	*Number of bays*	*Bay span [m]*	*Analysis notation*
EC8_2_2d	2	4.5 + 4.0	Planar	X	3	7.5	1
EC8_4_2d	4	3.5 + 3·3.0	Planar	X	2	4.0 and 5.0	2
EC8_5_2d	5	4.5 + 3·4.0	Planar	X	3	7.5	3
EC8_6_3d	6	3.7 + 5·3.0	Spatial	X	5	6.5	4
				Y	3	7.0	5
EC8_8_2d	8	4.5 + 7·4.0	Planar	X	3	7.5	6
EC8_8_3d	8	2.55 + 7·2.8	Spatial	X	3	6.0	7
				Y	2	6.0	8

Frames designed according to old codes

Six frames designed according to old codes (Kosič et al., 2014), ranging from 2 to 8 storeys, were analysed in the study. Four of them are planar and two spatial. Their notation, details about geometry and notation of analyses are shown in Table 2. The spatial frames were analysed in both orthogonal planes, therefore a total of 8 analyses were performed (noted with consecutive numbers from 1 to 8 in Table 2).

Table 2. Characteristics of frames designed according to old codes

Specimen notation	*Numb. of storeys*	*Storey height[m]*	*Planar / spatial*	*Direction*	*Number of bays*	*Bay span[m]*	*Analysis notation*
O_2_2d	2	4.5 + 4.0	Planar	X	3	7.5	1
O_4_2d	4	4·2.7	Planar	X	3	2.5 , 5.0	2
O_4_3d	4	4·3	Spatial	X	5	4.5	3
				Y	3	4.5	4
O_5_2d	5	4.5 + 4·4.0	Planar	X	3	7.5	5
O_7_3d	7	4.0 + 6·3.0	Spatial	X	2	5.8	6
				Y	5	4.0	7
O_8_2d	8	4.5 + 7·4.0	Planar	X	3	7.5	8

Wall systems

The array of analysed wall systems was divided in two sub-sets. The first represents wall systems containing walls with equal cross-sections. Since no redistribution of load between walls occurs during horizontal loading of such systems, the computational model consisted of a single multi-storey cantilever wall. A total of 24 single wall systems designed by Rejec et al. (2011) according to Eurocode 8 for high ductility level were addressed in the study. In all cases a 30 cm wide rectangular cross section was adopted. The storey height was 3.0 m. The following parameters were varied: (i) storey number n; (ii) wall length l_w; (iii) wall-to-floor ratio. The notation of walls and geometry details are provided in Table 3.

Table 3. Characteristics of single walls

Specimen notation	*Numb. of storeys*	*Wall-to-floor ratio*	*Wall length* l_w [m]	*Specimen notation*	*Numb. of storeys*	*Wall-to-floor ratio*	*Wall length* l_w [m]
1	4	1.5%	6.0	13	8	1.5%	3.0
2	4	1.5%	2.0	14	8	2.0%	6.0
3	4	2.0%	6.0	15	8	2.0%	3.0
4	4	2.0%	2.0	16	12	2.5%	6.0
5	4	1.5%	3.0	17	12	2.5%	4.5
6	4	2.0%	3.0	18	12	2.0%	6.0
7	6	1.5%	6.0	19	12	2.0%	4.5
8	6	1.5%	3.0	20	12	1.5%	6.0
9	6	2.0%	6.0	21	12	1.5%	4.5
10	6	2.0%	3.0	22	16	2.0%	6.0
11	6	2.0%	2.0	23	16	2.5%	6.0
12	8	1.5%	6.0	24	20	2.5%	8.0

The second set represents wall systems containing walls with different cross-sections. The computational models consisted of two or three unequal multi-storey walls. A total of 16 systems containing 2 walls and 1 system with 3 walls were addressed. All the examples were designed by Rejec (2011) according to Eurocode 8 for ductility class high.

All walls had a 30 cm wide rectangular cross section. The storey height was 3.0 m. The following parameters were varied: (i) storey number n; (ii) ratio between wall lengths; (iii) wall-to-floor ratio. The notation of systems containing two walls and their geometry details are provided in table 4. The system with 3 walls has 16 storeys, wall-to floor ratio 3.0% and wall lengths equalling 10, 6 and 3 meters.

Table 4. Characteristics of wall systems having walls with different lengths

Specimen notation	*Numb. of storeys*	*Wall-to-floor ratio*	*Long wall/ short wall*	*Wall length l_w* [m]	*Specimen notation*	*Numb. of storeys*	*Wall-to-floor ratio*	*Long wall/ short wall*	*Wall length l_w* [m]
1	4	1.5%	L.W.:	6.0	9	12	2.0%	L.W.:	6.0
			S.W.:	2.0				S.W.:	2.0
2	4	1.5%	L.W.:	6.0	10	12	2.5%	L.W.:	6.0
			S.W.:	4.0				S.W.:	2.0
3	6	1.5%	L.W.:	6.0	11	16	3.0%	L.W.:	10.0
			S.W.:	2.0				S.W.:	3.0
4	8	1.5%	L.W.:	6.0	12	16	3.0%	L.W.:	10.0
			S.W.:	2.0				S.W.:	5.0
5	8	1.5%	L.W.:	6.0	13	16	3.0%	L.W.:	10.0
			S.W.:	3.0				S.W.:	6.0
6	8	1.5%	L.W.:	6.0	14	16	3.0%	L.W.:	10.0
			S.W.:	4.0				S.W.:	7.0
7	8	1.5%	L.W.:	6.0	15	16	3.0%	L.W.:	10.0
			S.W.:	5.0				S.W.:	8.0
8	8	1.5%	L.W.:	10.0	16	16	3.0%	L.W.:	10.0
			S.W.:	3.0				S.W.:	9.0

Dual systems

One spatial dual system was addressed in the study. The system represents an abstracted sample for Eurocode 8 design (Fajfar and Kreslin, 2012). The structure has 6 storeys above ground (storey heights: 1 x 4 m + 5 x 3 m) and floor plan dimensions 30 m x 14 m. The bearing system for lateral loads along the long side of the structure (denoted with axis X) is provided by three frames and one wall with C-shaped cross section. Six frames, four rectangular walls and a C-shaped wall provide the support in Y direction. The cross-section dimensions of rectangular walls are 4 m x 0.3 m. The cross-section of C-shaped wall has outer dimension 4 m x 0.3 m and width 25 cm.

COMPUTATIONAL MODEL CHARACTERISTICS, DEFINITION OF DAMAGE STATES AND METHOD OF ANALYSES

Computational model characteristics

The computational models were composed by linear elastic line elements and non-linear rotational springs. Each structural element (beam, column or wall) was modelled with a linear elastic line element and two non-linear rotational springs at both ends, representing plastic hinges. The moment-rotation (M-θ) relationship for plastic hinges has a three-linear backbone (Figure 1-b), which includes softening. The characteristic points on the backbone are: (i) yielding (M_Y, θ_Y); (ii) maximum flexural capacity (M_C, θ_C); (iii) near collapse point (M_{NC}, θ_{NC}) and (iv) drop of capacity to zero (M_0=0,θ_0). The characteristic points were calculated using moment-curvature section analyses and empirically-based methods for determining the NC chord rotations of RC elements. CAE method (Peruš et al., 2006) was used in the case of columns and equation (A.1) from Eurocode 8-3 (CEN, 2005b) in the case of beams and walls. The initial stiffness of RC members was based on the 50% value of the cross section moment of inertia, as suggested by Eurocode 8. The data regarding the descending part of the loading curve are very limited and unreliable. The ratio between rotations θ_C and θ_0 (Figure 1-a) was arbitrarily chosen to be equal to 7 for beams and 3 for columns and walls. Note that such large numbers for θ_0/θ_C are reasonable only for the part between θ_C and θ_{NC}.

Linear elastic rule was adopted for the shear characteristics of structural members. Therefore no shear stiffness degradation or shear failure was considered in the analyses.

Definition of damage states

The damage level of individual member in the structure is represented by the observed rotation in the corresponding plastic hinges. The damage level is categorized according to five damage states. The damage states are defined according to the characteristic points on the hinge backbone:

i. No damage (grey area in figure 1-b). The rotation does not reach θ_Y;
ii. Moderate damage (green area in figure 1-b). The rotation exceeds θ_Y;
iii. Medium level of damage. The rotation surpasses the half-way point between θ_Y and θ_C, but does not exceed θ_C (yellow area in figure 1-b);
iv. Large level of damage. The rotation surpasses θ_C, but does not exceed θ_{NC} (red area in figure 1-b);
v. Very large level of damage. The rotation exceeds θ_{NC} (black area in figure 1-b).

Method of analyses

Pushover analysis was used. The shape of horizontal forces was proportional to the product between the floor masses and first mode shape. The influence of higher modes was neglected. Neither was considered the increase of seismic shear forces in walls due to dynamic amplification (Rejec et al., 2011). The models were loaded up to their NC limit state according to the first definition, i.e. until the strength of the structure dropped to 80% of the maximum strength. The analyses were performed in OpenSees (2013). Pre- and post- processing of the data was done using PBToolBox (Dolšek, 2010).

RESULTS OF ANALYSES

In this section several results of analyses are presented. All results apply to the deformation at the structure's NC state defined with 20% drop of strength (i.e. the first definition of the NC state at the level of the structure).

Characteristics of damage state at NC for frames designed according to modern codes

Figure 2 shows the damage state at NC limit state for two selected representative frames designed according to modern codes. The damage states of the members are denoted with appropriate colour scheme, defined in the previous paragraph. The distribution and level of damage for other analysed frames is very similar. The main characteristics of damage state at NC are:

a) The hinges at the bottom of the columns in the first storey surpassed θ_C, but did not exceed θ_{NC}.
b) Some damage of columns was observed at the middle-height of the structures. In none of the cases θ_C was exceeded.
c) All beams in the bottom half of the structures reached large level of damage (θ_C is exceeded). In the vast majority of cases the rotations exceeded θ_C and did not surpass θ_{NC}.
d) The beams at about two thirds of the structure height exhibited medium or moderate damage.
e) The deformation line is typical for frames: decreasing storey drifts from bottom to the top of the structure.

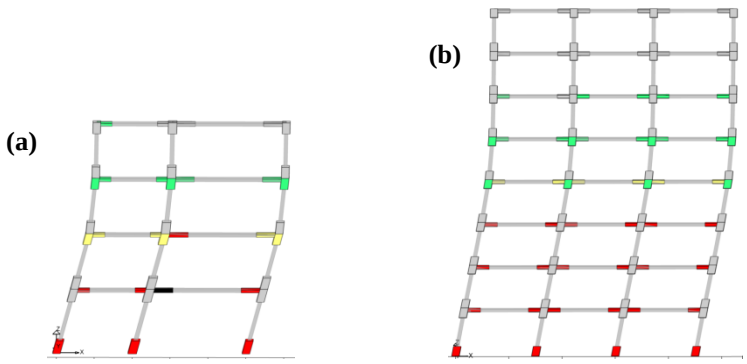

Figure 2: Damage state at NC for frames (a) EC8_4_2d and (b) EC8_8_2d

Characteristics of damage state at NC for frames designed according to old codes

In three cases a local (storey) mechanism was observed when loading old frames till NC. Figure 3 shows the damage states of the frames which exhibited local mechanism. They are denoted with the adopted colour scheme. The main characteristics of damage state at NC are:

a) In the case of frames O_2_2d and O_4_3d (X direction) the damage was completely confined to just one storey. On the other hand, the damage in frame O_4_2d was spread also to other storeys apart to the critical one.
b) The mechanism occurred in the third storey of the 4-storey frames and in the first storey of the 2-storey frame.
c) For O_2_2d and O_4_3d the rotations in the columns in the critical storey almost reached θ_{NC}. Most of the columns in the critical storey of O_4_2d surpassed θ_{NC}.

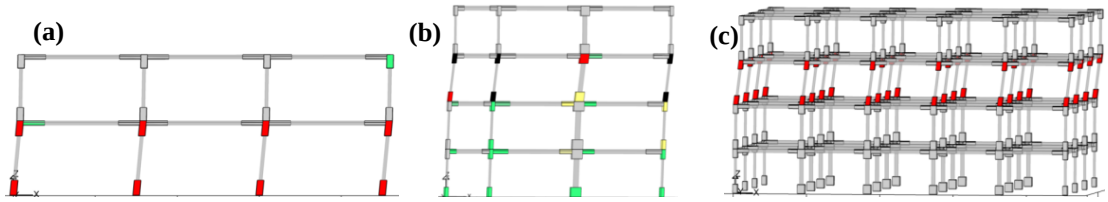

Figure 3. Frames that demonstrated a local mechanism: (a) O_2_2d, (b) O_4_2d, and (c) O_4_3d in X direction

Two examples of the frames that demonstrated global mechanism are shown in Figure 4. The distribution and level of damage for other old frames that exhibited global mechanism is very similar. The main characteristics of damage state at NC are:

a) The damage level and distribution resembles the damage in frames designed according to modern codes.
b) In the vast majority of cases the rotation in the bottom hinges of the first storey columns surpassed θ_C. Only the bottom columns of O_8_2d were less damaged (medium level of damage).
c) Some damage of columns was observed at the middle-height of the structures. Only the outer columns in O_4_3d and O_4_3d exhibited large level of damage.
d) All beams in the bottom half of the structures reached large level of damage (θ_C is exceeded). In the vast majority of cases the rotations exceeded θ_C and did not surpass θ_{NC}.
e) The beams at about two thirds of the structure height exhibited medium or moderate damage.

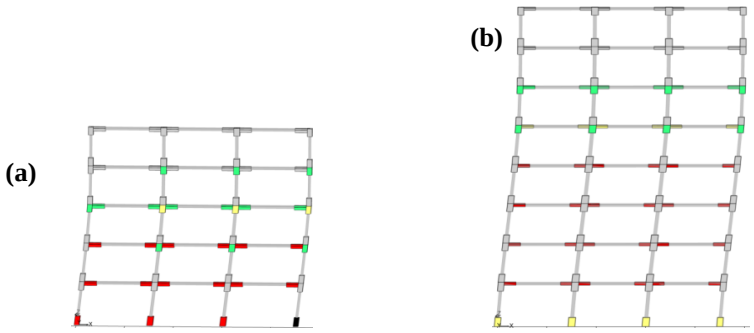

Figure 4. Examples of old frames that demonstrated global mechanism: (a) O_5_2d and (b) O_8_2d

Characteristics of damage state at NC for dual systems

Figure 5 shows the NC damage state of the analysed dual system. The damage characteristics are similar for both loading directions:

a) The rotations at the bottom of walls almost reached or surpassed θ_{NC}, when the walls were loaded in plane.
b) The columns were damaged only at the bottom. In most cases the damage was moderate. The rotations in some of the outer columns surpassed θ_C.

c) The beams, which are oriented in the direction of loading, exhibited large damage. In all the cases rotations surpassed θ_C and in some beams even θ_{NC}.

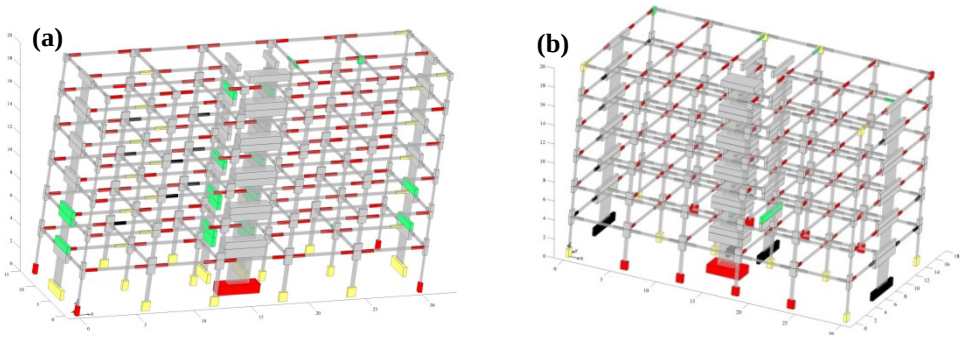

Figure 5. Damage state at NC for the analysed dual system: (a) loading in the X direction; (b) loading in the Y direction

Characteristics of damage state at NC for walls

All the analysed wall systems had the same damage pattern. The rotations at the bases of the walls surpassed θ_C but did not exceed θ_{NC}. The upper storeys were not damaged with the exception of the 20-storey wall, which also exhibited some minor yielding in the second storey. The drifts in all storeys were almost uniform. The maximal difference between drifts was 20% (20 storey wall).

Distribution of damage in elements according to the damage state categorization

The elements of the analysed structures were sorted into groups according to the damage state categorization. The results were normed and compared between examples. Figure 6 shows the damage distributions for frames designed according to modern codes. The designation on the vertical axis is in accordance to Table 1. In all the cases the columns at the bottom exhibit large damage (red notation), and some columns at mid-height suffer low or medium damage (green and yellow notation). Most of the columns remain undamaged (grey notation). Approximately half of the beams exhibit large or very large damage (rotations surpass θ_C; red and black notation). Around 15% of the beams are moderately damaged (yellow notation) and 25% exhibit little damage (green notation). In average 20% of beams remain undamaged.

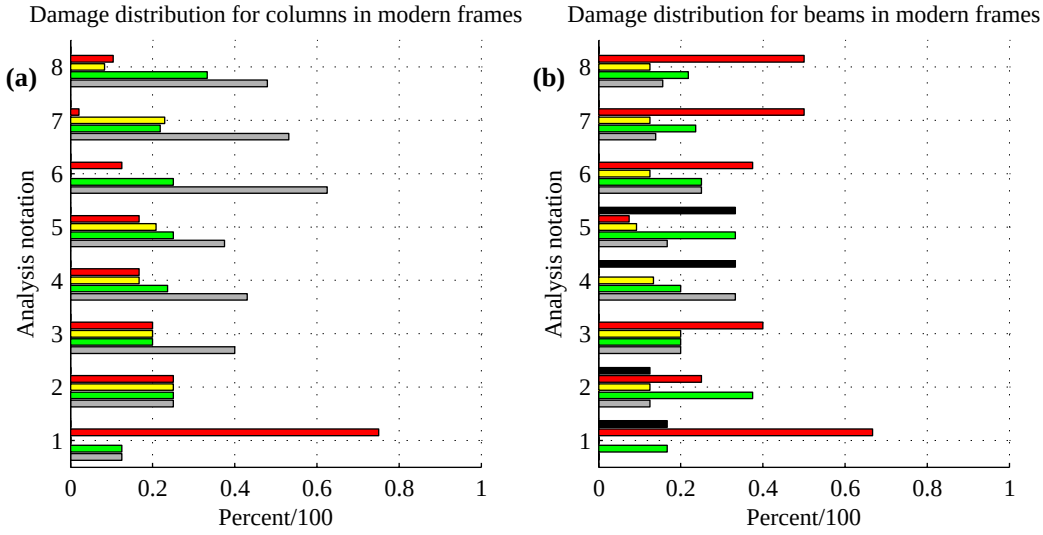

Figure 6. Distribution of damage in (a) columns and (b) beams for frames designed according to modern codes

Figure 7 shows the damage distributions for frames designed according to old codes. The designation on the vertical axis is in accordance to Table 2. The distribution of damage in beams clearly indicates that in cases 1, 2 and 3 the frames exhibited local mechanism. The beams were little

damaged and in one case even completely undamaged. For frames with global mechanism the distributions are very similar to frames designed according to modern codes. The column damage distribution in local mechanism frames is more uneven than in the case of frames with global mechanism. The dissimilarity of column damage distributions between global mechanism frames is more pronounced than in the case of modern frames.

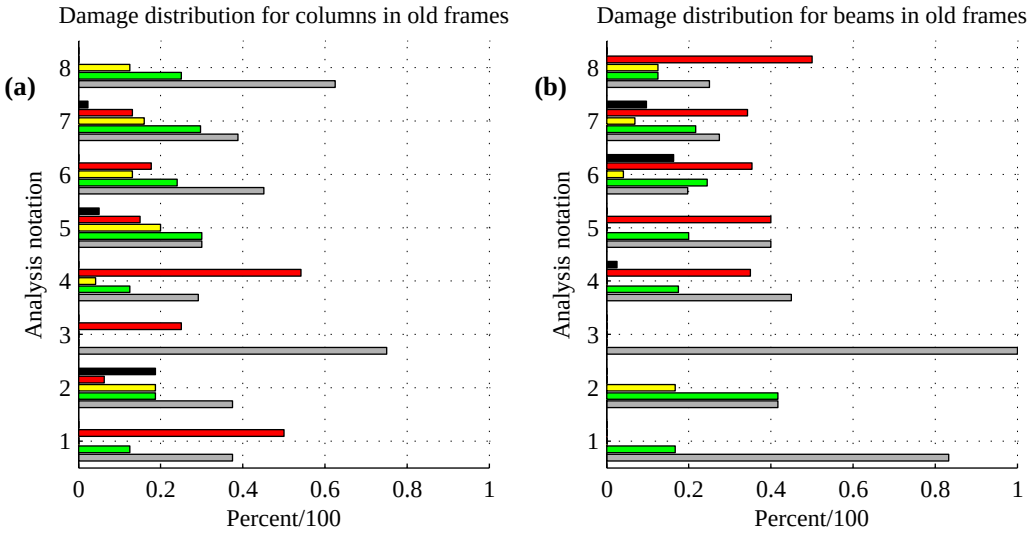

Figure 7. Distribution of damage in (a) columns and (b) beams for frames designed according to old codes

The damage distributions for the analysed dual system are shown in Figure 8. Loading in X direction and Y direction are labelled with number 1 and 2 respectively. The distributions are practically equal for both loading directions. All beams are largely damaged, 15% of them even surpassed the NC point. Most of the vertical elements are intact, as the damage is localized at the bottom (Figure 5).

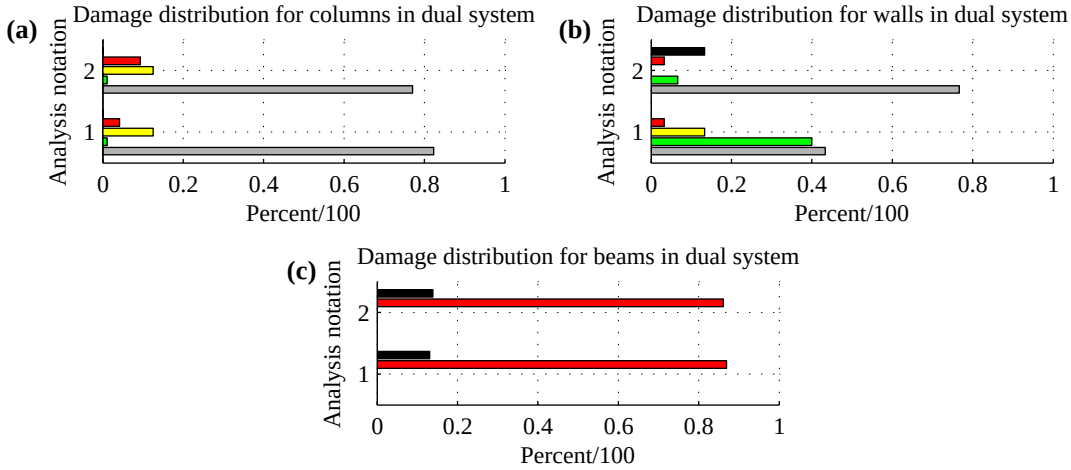

Figure 8. Distribution of damage in (a) columns, (b) walls and (c) beams for dual system

Overview of the maximal rotations in elements

The rotations in the most exposed elements at the structure's NC state (defined with 20% drop of strength) are compared with the elements' NC values. Figure 9 refers to frames designed according to modern codes. The sample of the most exposed elements consists of elements that developed rotations larger than θ_C. Mean and maximal values of ratios for columns ($\theta_{Col}/\theta_{Col,NC}$) and beams ($\theta_{Beam}/\theta_{Beam,NC}$) are plotted against the number of the storey. Ratios $\theta_{Col}/\theta_{Col,NC}$ are lower than 1 in all cases. For low-rise frames $\theta_{Col}/\theta_{Col,NC} \approx 0.9$. The value decreases for higher structures and reaches approximately 0.6

for 8-storey frames. Ratios for beams $\theta_{Beam}/\theta_{Beam,NC}$ are distributed between 0.6 and 1.2. The results indicate no correlation between $\theta_{Beam}/\theta_{Beam,NC}$ and the number of storeys.

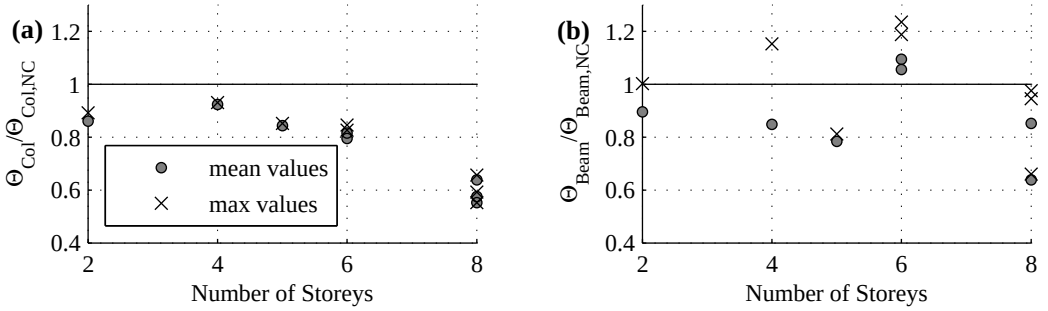

Figure 9. Ratios between the rotations in the hinges of the most exposed elements (at the structure's NC state) and their NC values: (a) columns $\theta_{Col}/\theta_{Col,NC}$; (b) beams $\theta_{Beam}/\theta_{Beam,NC}$. The results refer to frames designed according to modern codes

The ratios $\theta_{Col}/\theta_{Col,NC}$ and $\theta_{Beam}/\theta_{Beam,NC}$ for frames designed according to old codes are shown in figure 10. The sample of most exposed elements consists of elements that were categorised in the highest damage level state, observed in the corresponding frame. Ratios $\theta_{Col}/\theta_{Col,NC}$ range from 0.5 to 1.3. In 75% of cases $\max(\theta_{Col}/\theta_{Col,NC})$ equals to approximately 0.9. Only in one case, which is a frame with local mechanism, $\theta_{Col}/\theta_{Col,NC}$ surpassed the value of 1.0. The lowest value of $\max(\theta_{Col}/\theta_{Col,NC})$, which equals 0.55, was observed in the 8-storey frame. A weak trend of decreasing of $\theta_{Col}/\theta_{Col,NC}$ with the structure height exists. The ratios $\theta_{Beam}/\theta_{Beam,NC}$ for frames with global mechanism are near to 1.0 (ranging between 0.8 and 1.2). The beam ratios for frames with local mechanism are much lower and range up to 0.2.

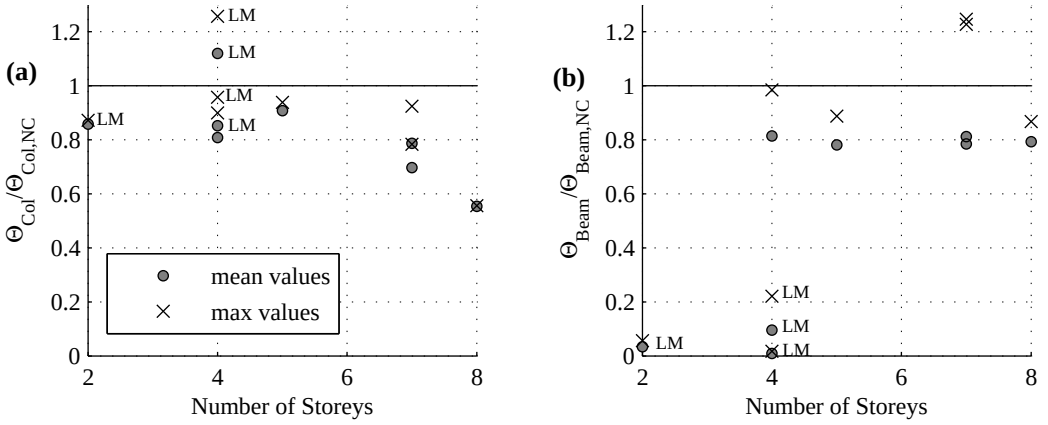

Figure 10. Ratios between the rotations in the hinges of the most exposed elements (at the structure's NC state) and their NC values: (a) columns $\theta_{Col}/\theta_{Col,NC}$; (b) beams $\theta_{Beam}/\theta_{Beam,NC}$. The results refer to frames designed according to old codes. LM indicates Local Mechanism

The $\theta_{Col}/\theta_{Col,NC}$ ratios for the dual system have the maximal value of about 0.95 and mean value of 0.65. The maximal values for walls ($\theta_{Wall}/\theta_{Wall,NC}$) are around 1.0. The ratios for beams range up to 1.5 with a mean value of 0.9.

Figure 11 shows the ratios $\theta_{Wall}/\theta_{Wall,NC}$ for wall systems. The ratios for single wall systems range from 0.8 to 1.0. A clear trend of decreasing $\theta_{Wall}/\theta_{Wall,NC}$ with increasing number of storeys is observed. The stiffest short systems have $\theta_{Wall}/\theta_{Wall,NC} \approx 1$. It seems that the ratio stabilizes at the value of 0.8, when the number of storey surpasses 12. Similar conclusions can be drawn for multiple wall systems. Values of $\max(\theta_{Wall}/\theta_{Wall,NC})$ range between 0.8 and 1. The stiffest short systems have $\theta_{Wall}/\theta_{Wall,NC} \approx 1$.

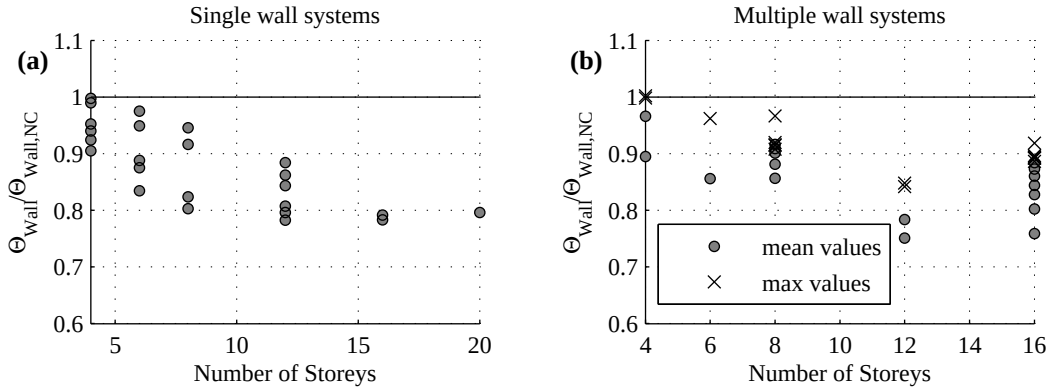

Figure 11. Ratios between the rotations in the hinges of the most exposed elements (at the structure's NC state) and their NC values: (a) Single wall systems; (b) Systems containing walls with different lengths. Note that for single wall systems the maximum and the mean values are equal

Ratios between the global drift and the maximum storey drift

Figure 12-a shows the ratios between the global drift Δ_{global} and the maximum storey drift $\Delta_{storey,max}$ for the frames designed according to new codes. Global drift Δ_{global} is defined as the ratio between the horizontal displacement at the top of the structure and the height of the structure. The storey drift is defined as the ratio between the (relative) storey displacement and storey height. For the two-storey frame $\Delta_{global}/\Delta_{storey,max}$ equals to about 1. All other frames have approximately the same ratio of about 0.6. The values for old frames are presented in figure 12-b. The values for frames with global mechanism are around 0.65. The values for frames with local mechanism are in general lower and have a wider range (from 0.3 to 0.6 for the two-storey frame).

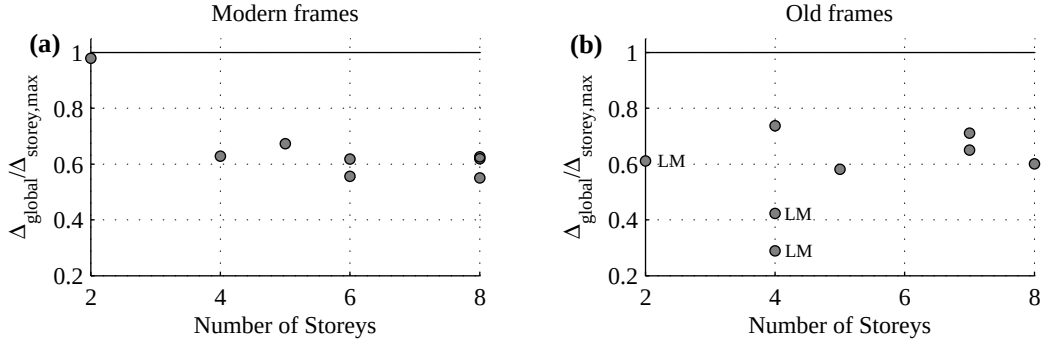

Figure 12. Ratios between the global drift and the maximum storey drift: (a) Frames designed according to new codes; (b) Frames designed according to old codes. LM indicates Local Mechanism

The values $\Delta_{global}/\Delta_{storey,max}$ for the dual system are approximately 1.0 for both loading direction. This means that the walls dictate the deformation shape of the whole system. The ratios for the analysed wall systems are plotted in Figure 13. In all cases $\Delta_{global}/\Delta_{storey,max}$ are a little bit below 1.0. A slight decrease of $\Delta_{global}/\Delta_{storey,max}$ with the increasing number of storeys can be observed.

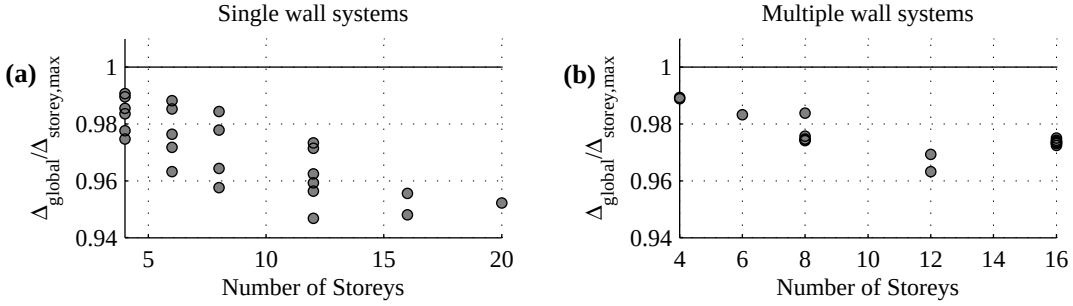

Figure 13. Ratios between the global drift and the maximum storey drift: (a) Single wall systems; (b) Systems containing walls with different lengths

Discussion of the results

The study showed that each structural type (frame, dual system or wall system), which fulfils the requirements of modern codes, has its typical damage pattern at the NC limit state. The damage mode of old frames, which demonstrate global mechanism, is similar to the one that is typical for modern frames. In the case of the local mechanism, the damage is concentrated in the respective storey.

The value 1.0 of the column or wall rotation ratio ($\theta_{Col}/\theta_{Col,NC}$ or $\theta_{Wall}/\theta_{Wall,NC}$) means that the structural NC limit state (defined with 20% drop of strength) coincides with the NC of the most exposed vertical element. This is approximately valid (approximately 10% deviation) only for low rise structures (e.g. up to 4 storeys). Column or wall rotation ratios of higher structures are lower than 1.0, meaning that the structural NC limit state is reached prior to the NC limit state of the first vertical element. The difference is particularly pronounced in the case of frames with larger number of stories. For wall systems up to 20 storeys and frames up to 6 storeys the difference between θ_{Col} (or θ_{Wall}) and $\theta_{Col,NC}$ (or $\theta_{Wall,NC}$) is less than 20%.

The trend of decreasing of $\theta_{Col}/\theta_{Col,NC}$ ($\theta_{Wall}/\theta_{Wall,NC}$) with the height of the structure indicates the influence of the second order effect (P-Δ effect). The effect is illustrated in Figure 14, where the pushover curves of a 4-storey and 20-storey single cantilever wall are shown. The square markers represent the limit states of the hinge at the base according to the adopted colour scheme (black is NC). The X marker indicates the drop of resistance for 20%, which is the structure NC state. Since the P-Δ effect "softens" the pushover curve, the structure NC state occurs prior to the element NC state.

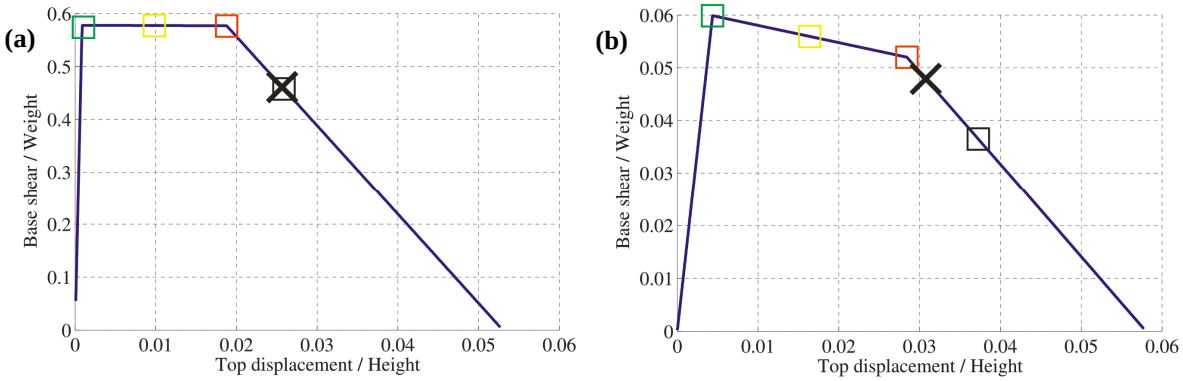

Figure 14. Pushover curves for (a) a 4-storey and (b) a 20-storey single cantilever wall. The square markers represent the limit states of the hinge at the base according to the adopted colour scheme (black is NC). The X marker indicates the drop of resistance for 20%, which is the structure NC state

The ratios between the global and maximum storey drifts ($\Delta_{global}/\Delta_{storey,max}$) amount to about 0.65 (with the exception of the two-storey modern frame) for frames with global mechanism, whereas much lower ratios apply to frames with local (storey) mechanism. The values $\Delta_{global}/\Delta_{storey,max}$ for wall systems are between 0.9 and 1.0. For the investigated dual system with the predominant influence of the walls the ratio is about 1.0.

CONCLUSIONS

Pushover analyses of a significant number of RC structures were performed up to their near collapse (NC) limit state, defined with 20% drop of the strength of the structure. The set of analysed structures included frames, wall systems and a dual system designed according to Eurocode 8, as well as frames designed according to old, obsolete codes. The damage at the NC limit state was documented.

The study showed that every structural type (frame, dual system or wall system), which fulfils the requirements of modern codes, has its typical damage pattern at the NC limit state. For modern frames, typically, about half of the beams exhibit large level of damage, whereas the columns are considerably damaged only at the base. On the other hand, the beams of the analysed dual system were highly damaged through the entire height of the structure. Wall systems sustained large damage only at the base. The damage mode of old frames, which demonstrate global mechanism, is similar to the

one that is typical for modern frames. Some old frames exhibited local (soft storey) mechanism, where the damage is concentrated in the weakest storey

The assumption that the structural NC limit state coincides with the NC of the most exposed vertical element is approximately valid only for low-rise buildings (up to 4 storeys). Higher buildings exhibit the structure NC limit state (defined with 20% drop of the strength) before the NC limit state of the most exposed vertical element is reached. The reason lies in the second order effect, which softens the pushover curve. Therefore the drop in the resistance of the structure occurs due to a combined effect of the deterioration of elements and of the second order effect.

For the investigated structures (with the exception of frames with local mechanisms) an approximately constant ratio between the global and maximum storey drift ($\Delta_{global}/\Delta_{storey,max}$) was observed. For frames that demonstrate global mechanism (modern frames and some old frames) the ratio amounts to about 0.65. For walls it ranges between 0.9 and 1.0. For dual systems with predominant wall behaviour the ratio $\Delta_{global}/\Delta_{storey,max}$ is about 1.0.

ACKNOWLEDGEMENT

The results presented in this paper are based on work continuously supported by the Slovenian Research Agency. This support is gratefully acknowledged.

REFERENCES

CEN (2005a) Eurocode 8—design of structures for earthquake resistance - Part 1: General rules, seismic actions and rules for buildings. European standard EN 1998-1, December 2004, European Committee for Standardization, Brussels

CEN (2005b) Eurocode 8—design of structures for earthquake resistance - Part 3: Assessment and retrofitting of buildings, December 2004, European Committee for Standardization, Brussels

Dolšek M (2010) "Development of computing environment for the seismic performance assessment of reinforced concrete frames by using simplified nonlinear models", *Bulletin of Earthquake Engineering*; 8(6):1309-1329

Fajfar P, Kreslin M (2012) "Introduction to the RC building example: Modeling and analysis of the design example", In: Acun B et al (eds.), *Eurocode 8: Seismic Design of Buildings, Worked examples*, (JCR Scientific and Technical Reports, ISSN 1831-9424, EUR 25204), Luxembourg: Publ. Office of the EU, JRC EU, pp. 25-52, http://eurocodes.jrc.ec.europa.eu/doc/WS_335/report/EC8_Seismic_Design_of_Buildings-Worked_examples.pdf

Kosič M, Fajfar P, Dolšek M (2014) "Approximate seismic risk assessment of building structures with explicit consideration of uncertainties", *Earthquake Engineering and Structural Dynamics*, Published online in Wiley Online Library (wileyonlinelibrary.com). DOI: 10.1002/eqe.2407

Lignos DG, Krawinkler H, Whittaker AS (2011) "Prediction and validation of sidesway collapse of two scale models of a 4-story steel moment frame", *Earthquake Engineering and Structural Dynamics*, 40:807–825

OpenSees (2013) Open System for Earthquake Engineering Simulation, Pacific Earthquake Engineering Research Center (PEER), Available from: http://opensees.berkeley.edu)

Peruš I, Poljanšek K, Fajfar P (2006) "Flexural deformation capacity of rectangular RC columns determined by the CAE method", *Earthquake Engineering and Structural Dynamics*, 35(12): 1453-1470

Rejec K (2011) Inelastic shear behaviour of RC structural walls under seismic conditions, Ph.D. Thesis, University of Ljubljana, Slovenia (in Slovenian), http://drugg.fgg.uni-lj.si/1821/1/ GRD_0217__Rejec.pdf

Rejec K, Isaković T, Fischinger M (2011) "Seismic shear force magnification in RC cantilever structural walls, designed according to Eurocode 8", *Bulletin of Earthquake Engineering*, 10(2): 567-586

Villaverde R (2007) "Methods to assess the seismic collapse capacity of building structures: state of the art", *Journal of Structural Engineering*; 133(1):57-66